RESEARCH PAPER

Green Synthesis and Optimization of Zinc Oxide Nanoparticles with Antimicrobial Properties

Shama Parveen[1*], Deep Narayan Maurya[2], Asha[3], Leena Nilesh Patil[4], Supriyatai K. Ahire[4*], Swapnil Ghanshyam Dhake[5], Hariom Mishra[6], Dhanashri Bhushan More[5]

[1*] Department of Chemistry, Faculty of Science, Motherhood University, Roorkee, India (Corresponding Author). Email: shamahussainktw@gmail.com

[2] Department of Chemistry, Faculty of Science, DN (P.G.) College Meerut, Uttar Pradesh, India

[3] Department of Chemistry, Guru Jambheshwar University of Science and Technology, Hisar, Haryana, India

[4] Department of Chemistry, School of Science, Sandip University, Nashik, Maharashtra, India

[4*] Department of Engineering Sciences and Humanities, Sandip Institute of Technology and Research Centre, Nashik, Maharashtra, India

[5] Department of Engineering Sciences and Humanities, Sandip Institute of Technology and Research Centre, Nashik, Maharashtra, India

[6] Department of Chemistry, Sunrise University, Alwar, Rajasthan - 301028, India

ABSTRACT

The phytochemical components of Leucas cephalotes were used in this study to create zinc oxide nanoparticles (ZnONPs) sustainably, and antibacterial investigations have all been used to characterize the ZnO NPs. A wurtzite hexagonal structure with an average crystallite size of 15.03 nm is revealed by XRD investigation. The zinc oxide nanoparticles' shape and elemental composition were investigated using SEM and EDX techniques. The ZnO nanoparticles' tetrapod-like structure was discovered through morphological investigations. FT-IR spectroscopy provided additional evidence that the nanoparticles' stabilizing functional groups are present. A study of UV-visible absorption revealed a 3.53 eV band gap. The antibacterial activity of ZnONPs was found to be significantly influenced by variations in their size and surface area-to-volume ratio. The positive diffusion method was used to evaluate ZnONPs' antibacterial activity. The findings demonstrated ZnONPs' strong broad-spectrum antibacterial capability by inhibiting the development of yeast and both Gram-positive and Gram-negative bacteria.

Keywords: Green synthesis, zinc oxide nanoparticles, characterization, antibacterial activity.

How to cite this article: Parveen S, Maurya DN, Asha, Patil LN, Ahire SK, Dhake SG, Mishra H, More DB. Green Synthesis and Optimization of Zinc Oxide Nanoparticles with Antimicrobial Properties. Int J Drug Deliv Technol. 2026;16(24s): 975-981. DOI: 10.25258/ijddt.16.24s.116

Source of support: Nil.

Conflict of interest: None

Introduction

Nanotechnology has emerged as a rapidly expanding field with significant relevance in diverse scientific domains, including chemistry, physics, biology, pharmacology, and information science [1–6]. Within the category of semiconductor nanomaterials, zinc oxide nanoparticles (ZnONPs) have gained notable prominence owing to their multifunctional characteristics, such as favorable semiconductor behavior, optical activity, pyroelectric and piezoelectric responses, and biodegradability. Zinc oxide is classified as an n-type semiconductor and is characterized by a wide band gap along with a strong excitonic binding energy [7–8]. Moreover, zinc oxide is listed by the U.S. Food and Drug Administration (FDA) as “Generally Recognized as Safe” (GRAS), reflecting its comparatively low toxicological risk [9]. These attributes have enabled the extensive application of ZnONPs in areas such as food packaging, electronic components, cosmetic formulations, sensing technologies, food safety monitoring, and catalytic processes.

In recent years, the strong antimicrobial efficacy exhibited by ZnONPs has generated substantial interest from both academic and industrial sectors, suggesting their potential role as promising substitutes for conventional antibiotic agents [10–11]. To date, a variety of physical and chemical synthesis techniques have been reported for producing ZnONPs with tailored sizes and morphologies, including hydrothermal processes, infrared-assisted synthesis, chemical vapor deposition, spray pyrolysis, and microwave-based sputtering methods [12–13]. Despite their effectiveness, many of these approaches

rely on toxic precursors, harsh reaction conditions, and high energy consumption, which limit their environmental compatibility and large-scale applicability [14–20].

As a result, increasing attention has been directed toward the development of environmentally sustainable and green synthesis strategies. Among these, plant extract–mediated synthesis has emerged as a cost-effective, eco-friendly, and efficient alternative for the fabrication of metal oxide nanoparticles. Although studies focusing on the biosynthesis of ZnONPs using plant resources are still comparatively scarce, existing reports confirm their successful synthesis and demonstrate encouraging biomedical potential [21]. Several plant species, such as *Brassica oleracea* var., *Cymbopogon citratus*, *Viscum album*, *Pelargonium zonale*, *Punica granatum*, *Aegle marmelos*, *Olea ferruginea*, and *Berberis vulgaris*, have been utilized as natural reducing and capping agents in the green synthesis of ZnONPs [22–29].

Experimental

Materials and Methods

Leucas cephalotes leaves were gathered from Kotdwar in Uttarakhand, India. All of the purest solvents and analytical grade zinc acetated hydrate $(ZnCH3COO)_2.2H_2O$ were purchased from Sigma-Aldrich (India).

Preparation of Leaf extract

After being completely cleaned, the Leucas cephalotes plant pieces were kept at room temperature. In a beaker with distilled water, about 8 g of dried Leucas cephalotes leaf powder was heated to 80–90 °C for an hour while being continuously stirred. After filtering the resultant combination, the extract was cooled to room temperature and kept for later use.

Green Synthesis of zinc oxide nanoparticles(ZnONPs)

An aqueous precursor solution of zinc chloride ($ZnCl_2$) was initially prepared at a concentration of 0.01 M for the synthesis of zinc oxide nanoparticles (ZnONPs). Separately diluted *Leucas cephalotes* leaf extract (6 mL) was then introduced slowly into the precursor solution under constant magnetic agitation, with dropwise addition carried out over a duration of 1 hour and 40 minutes. The progression of the reaction was evidenced by a gradual transition in solution color from brown to pale yellow, indicating nanoparticle formation. Following completion of the reaction, the mixture was allowed to equilibrate at room temperature. The synthesized nanoparticles were subsequently isolated via centrifugation at 1000 rpm for 15 minutes. To remove unreacted species and impurities, the collected precipitate was rinsed twice using distilled water and finally dried prior to further characterization analyses.

Characterisationstudies of ZnONPs

A variety of characterisation methods were used to precisely ascertain the physicochemical characteristics of the produced zinc oxide nanoparticles (ZnONPs). Their functional groups, surface charge, particle size distribution, chemical composition, and structural, morphological, electronic, and atomic properties were all examined using a variety of analytical techniques. UV–visible spectroscopy was used to examine the optical characteristics of the ZnONPs (Jasco V-650). A Zeta Sizer and Zeta Potential analyzer (Malvern Instruments, UK) was used to measure the particle size distribution and surface charge.

X-ray diffraction (XRD, Bruker D8 Advance) utilizing Cu Kα radiation was used to characterize the structure. Fourier Transform Infrared (FTIR) spectroscopy (Shimadzu IR Affinity-1A) was used to identify functional groups on the surface of the nanoparticles. Scanning Electron Microscopy (SEM, JEOL JEM-2100, Japan) was used to analyze the morphological features, and Energy-Dispersive X-ray (EDX) spectroscopy with an AMETEK TEAM V4.3 detector was used to confirm the elemental composition. The effective production and optimization of ZnONPs with desired physicochemical parameters were verified by various characterisation techniques taken together.

Antimicrobial Activity of ZnONPs.

The antibacterial activity of ZnONPs was examined in order to assess their potential medicinal uses. The agar well diffusion method, as outlined in earlier research, was used to evaluate the synthesized ZnONPs' antibacterial activity. Escherichia coli, Candida albicans, Bacillus subtilis, Pseudomonas aeruginosa, and Staphylococcus aureus were among the test microorganisms. The ZnONPs' antibacterial ability was assessed by measuring the bacterial growth inhibition zones.

Well diffusion method

A bacterial strain was grown in Muller-Hinton medium for an entire night at 37°C. The inculum was calibrated using a sterile sline and the CLSI (Clinical and LaboratoryStandards Institute) guidelines to get the desired density of 0.5 McFarland standard (1.5 x 108 CFU/mL). In order to achieve complete absorption, microbial inoculum was evenly

distributed across the tops of plates containing the growth environment and kept at room temperature for 15 minutes. Using a sterile cork borer, 7 mm-diameter holes have been aseptically punched onto inoculation plates, and 50 ul of a nanoparticle solution has been added to each well. After that, bacteria-filled agar plates were incubated at 37°C for 24 hours. In accordance with the diameter (mm) of the inhibition zones formed due to the diffusion of ZnONPs in the medium and the subsequent inhibition of microbial growth, the antimicrobial activity of the produced nanoparticles was assessed.

Mechanism of Antibacterial Action of ZnONPs

The antibacterial activity of zinc oxide nanoparticles (ZnONPs) is governed by multiple synergistic mechanisms. One of the primary mechanisms involves the generation of reactive oxygen species (ROS), such as hydrogen peroxide, superoxide radicals, and hydroxyl radicals, which induce oxidative stress within bacterial cells. These ROS can damage cellular components including proteins, lipids, and nucleic acids, ultimately leading to cell death. Additionally, the small size and high surface area of ZnONPs facilitate their close interaction with bacterial cell membranes, resulting in membrane disruption, increased permeability, and leakage of intracellular contents. The release of Zn^{2+} ions further contributes to antibacterial activity by interfering with enzymatic systems and metabolic pathways. Collectively, these mechanisms account for the broad-spectrum antibacterial efficacy of ZnONPs, particularly against Gram-negative bacteria.

RESULTS AND DISCUSSION

UV. VisibleSpectrumanalysis

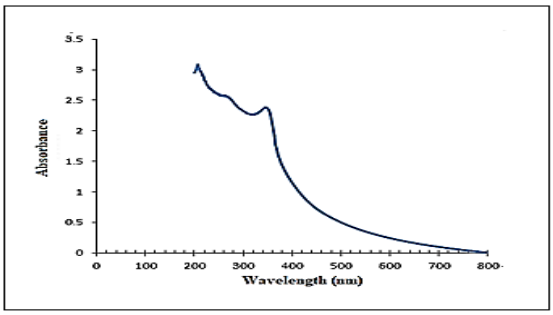

Fig. 1; FTIR Spectra ZnONPs using *Leucas Cephalotes* leaf extract

UV–visible spectroscopy was employed to evaluate the optical properties of the synthesized zinc oxide nanoparticles (ZnONPs). The UV–Vis absorption spectrum of ZnONPs (Fig. 1) displayed a prominent absorption peak at 349 nm, which is attributed to the electronic band-gap transition between the valence and conduction bands. The presence of this characteristic absorption peak confirms the successful formation of ZnONPs synthesized using *Leucas cephalotes* leaf extract. The optical band gap energy of the ZnONPs was calculated to be 3.53 eV. The slight reduction in band gap energy compared to bulk ZnO can be associated with intrinsic structural defects, such as oxygen vacancies and zinc interstitials, which introduce localized energy states within the band structure.

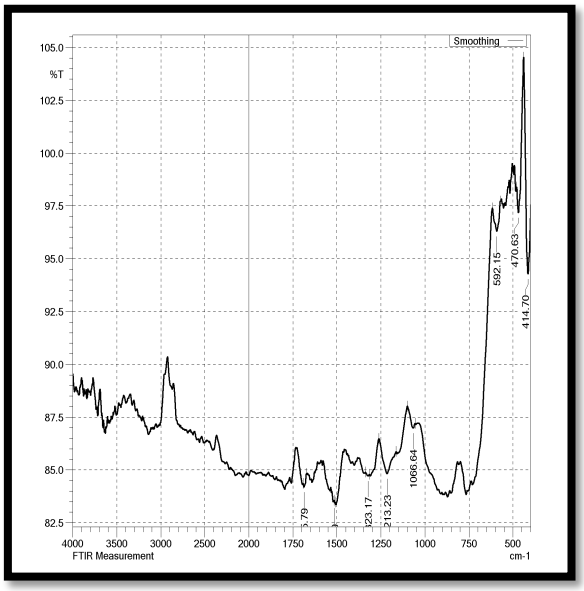

Fig. 2; FTIR Spectra ZnONPs using *Leucas Cephalotes* leaf extract

FT-IR

The FTIR spectrum recorded in the range of 4000–400 cm^{-1} reveals the presence of multiple functional groups and confirms the successful formation of the synthesized material. A broad absorption band observed around 3400–3200 cm^{-1} is attributed to O–H stretching vibrations, indicating surface-adsorbed moisture or hydroxyl groups, while weak bands near 2920–2850 cm^{-1} correspond to C–H stretching vibrations of residual organic components. The appearance of an absorption band in the region of 1735–1700 cm^{-1} suggests C=O stretching vibrations, whereas bands around 1500–1450 cm^{-1} are associated with C=C stretching or CH_2/CH_3 bending modes. Distinct peaks at approximately 1323 cm^{-1} and 1213 cm^{-1} are assigned to C–O stretching or metal–oxygen–carbon linkages, indicating strong interaction between organic and inorganic phases. A prominent band at about 1066 cm^{-1} corresponds to C–O–C or metal–oxygen vibrations, reflecting the formation of a stable bonding network. Furthermore, intense absorption bands in the low wavenumber region at

around 592, 470, and 414 cm^{-1} are attributed to metal–oxygen stretching vibrations, confirming the formation of the inorganic framework and validating the successful synthesis of the material.

XRD

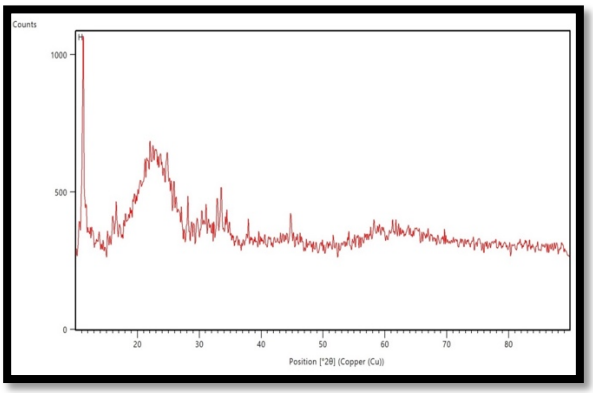

Fig. 3; XRD Spectra FeONPs using *Leucas Cephalotes* leaf extract

The XRD pattern of the biosynthesized ZnONPs exhibits characteristic diffraction peaks at 2θ values of approximately 31.7°, 34.4°, and 36.2°, which are indexed to the (100), (002), and (101) crystallographic planes of hexagonal wurtzite ZnO (JCPDS No. 36-1451), respectively. The presence of these indexed planes confirms the successful formation of crystalline ZnO nanoparticles. The broad nature of the diffraction peaks indicates the nanoscale dimensions and defect-rich structure of the synthesized ZnONPs, which is typical for plant-mediated green synthesis routes.

The Debye Scherrer formula (Yahyaoui, Amina, et al., 2017) was used to calculate the diameter of the synthesized zinc oxide nanoparticles. The full width at half-maximum of the diffraction peak related to the aircraft at 002 and 100. The sample had a median size of 15.03 nm, according to examination.

Zeta potential Analysis of zinc oxide nanoparticles (ZnONPs)

The charge stability of ZnONPs produced from *Leucas cephalotes*leaf extract can be analysed using the Zeta potential. The zeta capability denotes the charge on the surface. Demonstrate that the zeta potentials of ZnONPs dispersed in water were determined to be -39.76 mV. The zeta potential at its maximum clearly shows good stability.

SEM Morphological Analysis

Utilizing SEM, the shape and morphology were examined (JEOL JEM 2100, Japan). The formation of zinc oxide produced by *Leucas cephalotes* leaf extract and its morphological dimensions were investigated using SEM. The SEM images of ZnO nanoparticles taken at various magnifications are shown in Fig. 4. these images demonstrate how ZnO-NPs develop. These images support the nanoparticles' approximative tetrapod structure, and most of the particles show some faceting. These tetrapod similar tooles research (Yan, L., Uddin, A., & Wang, H. (2015). A high depth of field in SEM micrographs produces a distinctive 3D look that is helpful for comprehending the surface structure of NPs.

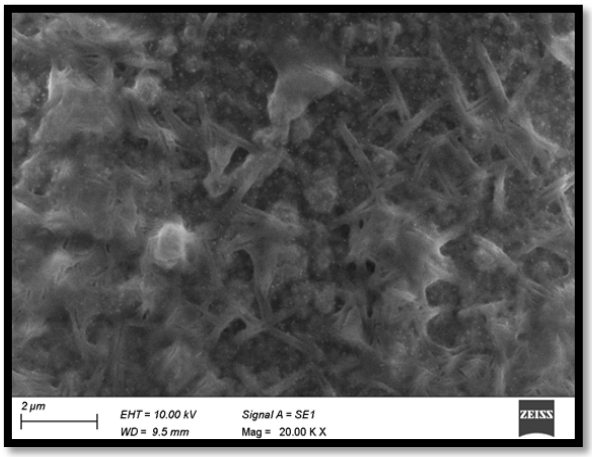

(a)

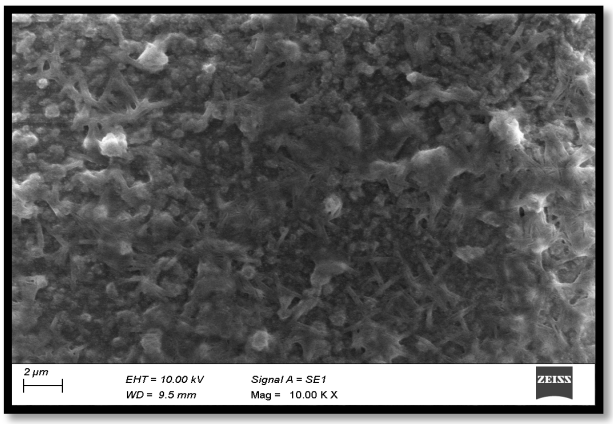

(b)

Fig. 4; Depicts the SEM photo of ZnONPs made from *Leucas cephalotes* leaf extract of (a) using 20 KX (b) using 10 KX

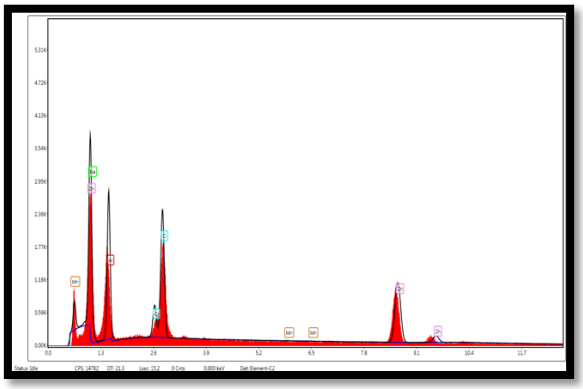

Fig. 5; Show represents the EDAX image of ZnONPs using leaf extract of *Leucas cephalotes*

A high depth of field in SEM micrographs produces a distinctive 3D look that is helpful for comprehending the sample's surface chemistry. The investigation using EDX analysis establishes that the grains are metallic ZnO-NPs and are crystalline in character (Fig. 5). Zinc oxide weight percentage was detected by EDX at 51.11%, 21.86% and 27.03% other elements respectively.

Antimicrobial activity

Table 1. Shows the inhibition zones for nanoparticles of zinc oxide produced using the Agar well diffusion method.

1.	Samples name	Staphylococcus aureus Inhibition zone (mm)	Bacillus Subtilis Inhibition zone (mm)	Escherichia coli. Inhibition zone (mm)	Pseudomonas aeruginosa (MTCC) inhibition zone (mm)	Candida albicans (MTCC) Inhibition zone (mm)
	ZnO NPs (created by leaf extract by (*Leucas Cephalotes*)	**13**	**NI**	**18**	**20**	**NI**

The antimicrobial activity of the biosynthesized ZnONPs was evaluated against selected Gram-positive, Gram-negative, and fungal strains using the zone of inhibition method. The ZnONPs exhibited notable antibacterial activity against *Staphylococcus aureus* (13 mm), *Escherichia coli* (18 mm), and *Pseudomonas aeruginosa* (20 mm). Among the tested microorganisms, *Pseudomonas aeruginosa* showed the highest sensitivity toward ZnONPs. In contrast, no inhibitory activity was observed against *Bacillus subtilis* and *Candida albicans*.

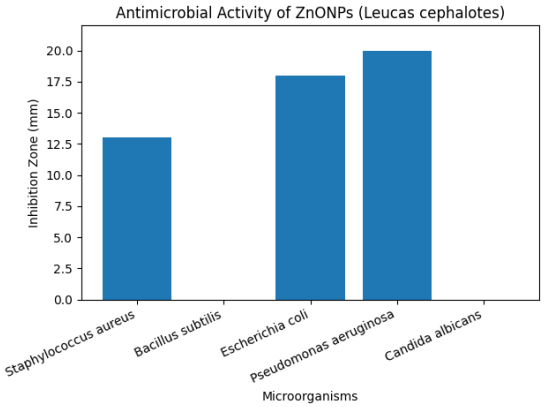

Fig. 6; Bar Graph Shows Antimicrobial Activity Of ZnONPs

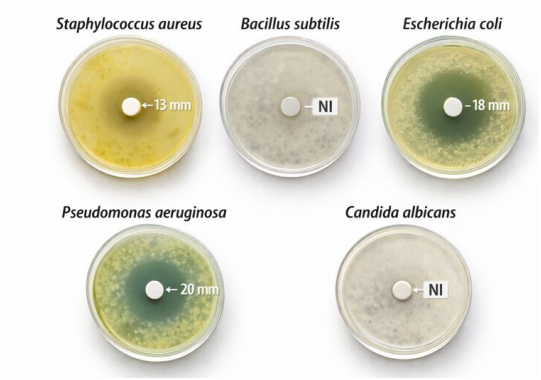

Fig.7; Antimicrobial activity of ZnONPs

The enhanced antibacterial performance of ZnONPs may be attributed to their nanoscale size, high surface area, and the generation of reactive oxygen species (ROS), which can disrupt bacterial cell membranes, proteins, and DNA. The variation in inhibition zones among different microbial strains can be related to differences in cell wall structure and permeability between Gram-positive and Gram-negative bacteria, as well as the inherent resistance mechanisms of fungal cells.

Conclusion

Zinc oxide nanoparticles (ZnONPs) were successfully synthesized via a green and sustainable approach using *Leucas cephalotes* leaf extract. UV–visible analysis confirmed nanoparticle formation with a characteristic absorption at 349 nm and an optical band gap of 3.53 eV. FTIR results demonstrated the involvement of plant-derived phytochemicals in the reduction and stabilization of ZnONPs, while XRD analysis confirmed their crystalline hexagonal wurtzite structure with an average crystallite size of approximately 15 nm. The high negative zeta potential (−39.76 mV) indicated excellent colloidal stability. SEM analysis revealed predominantly

tetrapod-like nanostructures with well-defined facets. Overall, the results establish *Leucas cephalotes*–mediated synthesis as an efficient and eco-friendly route for producing stable and crystalline ZnONPs with promising potential for biomedical, antibacterial, and environmental applications.

Aknowledgements

In order to complete this work, the authors would like to express their gratitude to the Department of Chemistry at Motherhood University, Roorkee, Uttarakhand.

Conflict Of Interest

The authors declare that there is no conflict of interest.

References

1. A. L. Porter, J. Youtie, How interdisciplinary is nanotechnology? *J. Nanopart. Res.,***11**, 1023–1041 (2009).
2. M. Govindarajan, G. Benelli, *Ecotoxicol. Environ. Saf.,***133**, 395–402 (2016).
3. M. Govindarajan, G. Benelli, *J. Clust. Sci.,***28**, 15–36 (2017).
4. C. Balalakshmi, K. Gopinath, M. Govindarajan, R. Lokesh, A. Arumugam, N. S. Alharbi,S. Kadaikunnan, J. M. Khaled, G. Benelli, *J. Photochem. Photobiol B*,**173**, 598–605 (2017).
5. M. Divya, B. Vaseeharan, M. Abinaya, S. Vijayakumar, M. Govindarajan, N. S. Alharbi, S. Kadaikunnan, J. M. Khaled, G. Benelli, *J. Photochem. Photobiol B* **178**, 211–218 (2018).
6. B. A. Fahimmunisha, R. Ishwarya, M. S. AlSalhi, S. Devanesan, M. Govindarajan, B. Vaseeharan,*J. Drug Deliv. Sci. Technol.,***55**. (2020)
7. D. Suresh, R.M. Shobharani, P.C. Nethravathi, M.A.P. Kumar, H. Nagabhushana,141, 128–134 (2015).
8. R. Gill, S. Ghosh, A. Sharma, D. Kumar, V.H. Nguyen, D.V.N. Vo, T.D. Pham,P. Kumar, *Mater. Lett.,***277**, 128295 (2020).
9. M. Chennimalai, V. Vijayalakshmi, T.S. Senthil, N. Sivakumar, *Mater. Today.,***47**, 1842–1846 (2021).
10. A. Krol, V. Railean-Plugaru, P. Pomastowski, B. Buszewski, *Phytochem. Lett.,***31**, 170–180 (2019).
11. H. Singh, A. Kumar, A. Thakur, P. Kumar, V.H. Nguyen, D.V.N. Vo, A. Sharma,D. Kumar, *Top. Catal.,* 63, 1097–1108 (2020).
12. D. Skoda, P. Urbanek, J. Sevcik, L. Munster, J. Antos, I. Kuritka, *Mater. Sci. Eng. B.,* 232–235, 22–32 (2018).
13. S. Bhat, S.V. Shrisha, K.G. Naik, *Arch. Phy. Res.,***4**, 61–66 (2013).
14. S. S. Kumar, P. Venkateswarlu, V. R. Rao, G. N. Rao, G.N, *Int. Nano Lett.,***3**, 30 (2013).
15. P. Suganya, B. Vaseeharan, S. Vijayakumar, B. Balan, M. Govindarajan, N. S. Alharbi, S. Kadaikunnan, J. M. Khaled, G. Benelli, *J. Photochem. Photobiol B.,***173**, 404–411 (2017).
16. R. Ishwarya,B. Vaseeharan, R. Anuradha, R. Rekha, M. Govindarajan, N. S,Alharbi, S. Kadaikunnan, J. M. Khaled, G. Benelli,*J. Photochem. Photobiol B.,***174**, 133–143 (2017a).
17. R. Thaya, B. Vaseeharan, J. Sivakamavalli, A. Iswarya, M. Govindarajan, N. S. Alharbi, S. Kadaikunnan, M. N. Al-anbr, J. M. Khaled, G. Benelli, *Microb. Pathoge.,***114**, 17–24 (2018).
18. V. Karthika, M.S. AlSalhi, S. Devanesan, K. Gopinath, A. Arumugam, M. Govindarajan, *Sci. Rep.,***10**, 1 (2020). G. Kasi, J. Seo, Influence of Mg doping on the structural, 2019
19. R. M. Kiriyanthan, S. A. Sharmili, R. Balaji, S. Jayashree, S.Mahboob, K. A. Al-Ghanim, F. Al-Misned, Z. Ahmed, M. Govindarajan, B. Vaseeharan, *Photodiagn. Photodyn. Thar.,***32** (2020).
20. M. MuthuKathija, M. S. M. Badhusha, & V. Rama, V. *Applied Surface Science Advances.*, **15**, 100400 (2023).
21. H. S. Elshafie, A. Osman, M. M. El-Saber, ,I. Camele, I., & E. Abbas, *The Plant Pathology Journal.*, **39**(3), 265 (2023).
22. U. Manojkumar, D. Kaliannan, V. Srinivasan, B. Balasubramanian, H. Kamyab, Z. H. Mussa, & S. Palaninaicker, S, *Chemosphere.*, *323*, 138263, (2023).
23. Y. H. I.Mohammed, S. Alghamdi, H. A. Alzahrani, B. Jabbar, D. Marghani, S. Beigh & W. N. Hozzein,. *ACS Omega*., (2023).
24. W. Mushtaq, M. Ishtiaq,M. Maqbool, M. W. Mazhar, R. Casini, A. M. Abd-ElGawad, & H. O. Elansary, *Plants.*, 12(11), 2130 (2023).
25. A. Vahidi, H. Vaghari, Y. Najian, M. Najian, H. Jafarizadeh-Malmiri, H, *Green Process. Synth.,***8**, 302–308 (2019).

26. E. Karaköse, H. Çolak, F. Duman, F, Green Process. Synth., 6, 317–323 (2017).
27. J. Fowsiya, I. V. Asharani, S. Mohapatra, A. Eshapula, P. Mohi, N. Thakar, S. Monad, G. Madhumitha, *Green Process Synth.*, **8**, 488–495 (2019).
28. A. Hussain, A. Mehmood, G. Murtaza, K. Ahmad, A., Ulfat, M. Khan, T. Ullah, T, *Green Process. Synth.,***9**, 451–461 (2020).
29. Y. Anzabi, *Green Process. Synth.,*7, 114–121 (2018).
30. I. Kim, K., Viswanathan, G. Kasi, K. Sadeghi, S. Thanakkasaranee, J.,& Seo, *Polymers*, **11**(9), 1427 (2019).
31. Y., L., A. Uddin, H. Wang. *Nanomaterials and Nanotechnology* **5** (2015): 19.
32. K., I., K. Viswanathan, G. Kasi, K. Sadeghi, S. Thanakkasaranee, J. Seo. *Polymers* 11, no. 9 (2019): 1427.